www.ksmrm.org JKSMRM 16(3) : 226-235, 2012
Print ISSN 1226-9751

Original Article

Differentitation between Primary Central Nervous System Lymphoma and Glioblastoma: Added Value of Quantitative Analysis of CT Attenuation and Apparent Diffusion Coefficient

Seung Choul Lee[1], Won-Jin Moon[1], Jin Woo Choi[1], Hong Gee Roh[1], So hyeon Bak[1], Jeong Geun Yi[1], Yoo Jeong Yim[2], En Chul Chung[3]

[1]Department of Radiology, Konkuk University School of Medicine, Seoul, Korea
[2]Department of Radiology, Konkuk University Medical Center, Seoul, Korea
[3]Department of Radiology, Kangbuk Samsung Hospital, Sungkyunkwan University School of Medicine, Seoul, Korea

Purpose : Purpose of this study was to determine if quantitative measures of CT attenuation and ADC values in combination with conventional imaging features can differentiate primary central nervous system lymphoma (PCNSL) and glioblastoma (GBM).

Materials and Methods: Twenty-six patients with histologically-proven GBM (14 men and 12 women; median age, 50 years; age range, 22 – 73 years) and 14 patients with PCNSL (11 men and 3 women; median age, 61 years; age range, 41 – 74 years) were enrolled. Maximum CT attenuation, minimum ADC, and lesion to normal parenchyma minimum ADC ratios were measured in solid tumor regions. Conventional imaging features were evaluated for the following: ill-defined margin, homogeneous enhancement pattern, degree of necrosis, extent of tumor involvement and multiplicity. The Mann-Whitney test was used to compare maximum CT attenuation and minimum ADC values for PCNSL and GBM. Fisher's exact test was used to evaluate relationships between pathologic diagnoses and imaging features.

Results: The CT attenuations were similar for PCNSL and GBM (37.84 $\pm$ 6.90 HU versus 37.00 $\pm$ 5.54 HU, p = 0.68), but minimum ADC and minimum ADC ratio were significant lower in PCNSL than in GBM (595.01 $\pm$ 228.28 10^{-6} mm^2/s versus 736.52 $\pm$ 162.05 10^{-6} mm^2/s; p = 0.028, 0.87 $\pm$ 0.26 versus 1.14 $\pm$ 0.29; p = 0.007). PCNSL showed greater homogeneous enhancement and smaller necrotic areas than GBM (p = 0.003 and p < 0.001, respectively) and was more likely to have multiple tumors than GBM (p = 0.039). When necrotic PCNSL (n = 4) and necrotic GBM (n = 24) were compared, minimum ADC and minimum ADC ratios were also significantly lower in PCNSL, but CT attenuation were not.

Conclusion: Although CT attenuation does not provide valuable information, minimum ADC and minimum ADC ratio and some imaging features can aid the differentiation of PCNSL and GBM.

Index words : Central Nervous System · Lymphoma · Glioblastoma · Computed tomography (CT) Diffusion weighted imaging (DWI)

• Received; August 27, 2012 • Revised; October 23, 2012
• Accepted; October 28, 2012
This study was supported by Konkuk University in 2012
Corresponding author : Won-Jin Moon, M.D., Ph.D.
Department of Radiology, Konkuk University Medical Center, Konkuk University School of Medicine, 4-12, Hwayang-dong, Gwanjin-gu, Seoul, 143-792, Korea.
Tel. 82-2-2030-5499, Fax. 82-2-2030-5549
E-mail : mdmoonwj@naver.com, mdmoonwj@kuh.ac.kr

INTRODUCTION

The incidence of primary central nervous system lymphoma (PCNSL) is increasing because of population aging and imaging modality advancements, and currently, PCNSL represents 1 – 5% of all brain tumors (1, 2). Systemic chemotherapy with or without

radiation therapy is the mainstay in treatment for PCNSL (3, 4). Thus, radical surgical resection is not indicated for presumable PCNSL because only a brain biopsy is needed to make a pathologic diagnosis (5).

Glioblastomas (GBMs) are the most common malignant tumors in adults and are also showing an increasing trend due to population aging. Although, the prognosis of GBMs has been much improved by the recent development of the DNA alkylating agent temozolamide (6), wide surgical resection is the key to prolonged survival and prognosis for GBM (7, 8).

In immunocompetent patients, PCNSL lesions are isoattenuated or hyperattenuated on unenhanced CT images and show marked contrast enhancement on both CT and MR images (9–11). However, these findings are nonspecific and are also observed for GBM. Although perfusion-weighted imaging (PWI) may aid the differentiation of PCNSL and GBM by demonstrating a low cerebral blood volume in PCNSL (11, 12), this imaging method has several disadvantages, such as, relatively low resolution, sensitivity to magnetic susceptibility artifacts, and the use of gadolinium contrast agent (2, 13).

Diffusion-weighted imaging (DWI) is not only one of the advanced imaging methods but also is a straightforward and easily applied method in clinical practice, unlike PWI or MR spectroscopy. DWI measures the diffusion property of water molecules within biologic tissues, and thus, intratumoral apparent diffusion coefficients (ADCs) are considered imaging markers of cellularity for various tumors (14). Furthermore, some authors have found that PCNSL lesions have lower ADC values than GBM lesions (15, 16).

Because CT attenuation is directly proportional to electron density of the tissue and the atomic number of the tissue composition in a given volume, CT attenuation is correlated with tumor cellularity (17), and can be used as an imaging marker for tumor cellularity. However, to the best of our knowledge, there has been no study on quantitative analysis on PCNSL and GBM, except one having briefly addressed the quantification of CT attenuation of GBM and PCNSL on a table (18). Unfortunately, the authors did not discuss the CT attenuations of the two tumors groups in detail because differentiation between PCNSL and GBM were not their subject (18). Nevertheless, the attenuations of lesions on unenhanced CT could provide attractive markers, in terms of, simplicity, cost-effectiveness, and feasibility, if they could be used to differentiate PCNSL and GBM accurately.

We hypothesized that unlike heterogeneous, loosely packed GBMs, homogeneous densely packed PCNSLs would have higher attenuations on unenhanced CT images and lower ADC values on DW images. In addition we hypothesized that conventional imaging features can differentiate PCNSL and GBM, and that quantitative analysis of CT attenuation and ADC values help distinguish PCNSL from GBM in case of PCNSL having uncommon conventional features, such as PCNSL with necrosis. Hence, the purpose of this study was to determine whether quantitative measures of CT attenuation and ADC, in combination with conventional imaging features, can differentiate PCNSL and GBM.

MATERIALS AND METHODS

This retrospective study was approved by the institutional review boards of the hospitals involved; the requirement for informed consent was waived.

Patients

Twenty consecutive patients with pathologically proven PCNSL were recruited between March 2006 and December 2010 at two university-affiliated institutions. Those patients that had undergone both unenhanced CT and conventional magnetic resonance (MR) imaging with DWI before surgery or surgical biopsy were considered. Two of the 26 without initial unenhanced CT images, and 6 without DW images were excluded. Finally 14 patients with PCNSL (11 men and 3 women; median age, 61 years; age range, 41 – 74 years; 13 diffuse large B cell lymphoma, 1 extranodal NK/T-cell lymphoma, nasal type) were included in the study.

For comparison purposes, 32 patients with pathologically proven GBM that enrolled at one of the institutions between March 2006 and December 2009 were also considered. Four patients without an initial unenhanced CT images and two without DW images were excluded. Thus, 26 patients with GBM (14 men and 12 women; median age, 50 years; age range, 22 – 73 years) were finally included for analysis.

CT imaging

All CT scans were obtained using a helical CT scanner (LightSpeed, GE Medical Systems, Milwaukee, WI; or a Definition, Siemens Medical Systems, Erlangen, Germany). The scanning parameters for unenhanced CT were 120 kVp and 330 mAs with an image matrix of 512 × 512, a 23- or 24-cm field of view, and a section thickness of 5-mm.

Conventional MRI and diffusion weighted MR imaging

MR examinations were conducted using a 1.5T unit (Intera, Philips Medical Systems, Best, the Netherlands) (5 patients with PCNSL) or a 3T unit (SignaHDxt, GE Medical Systems, Milwaukee, WI, USA) (9 patients with PCNSL and all 26 patients with GBM).

MRI examinations included the following sequences: axial T1-weighted spin-echo (TR/TE, 500/8–15 ms; FOV, 22 – 24 cm; section thickness/section gap, 5 mm/2 mm; matrix, 320 × 192) or axial T1-inversion (TR/effected TE/inversion time (TI), 2468/12/920 ms; FOV, 22 cm; ST/IG, 5 mm/2 mm; matrix, 512 × 224), axial T2-weighted fast-spin echo (TR/effected TE, 4000/85–100; FOV, 22–24 cm; ST/IG, 5 mm/2 mm; matrix, 384 × 256 or 384 × 384), axial FLAIR (TR/TE/TI, 10000–11000/105/2600 ms; FOV, 22–24 cm; ST/IG, 5 mm/2 mm; matrix, 384 × 224, axial T2*-weighted gradient-echo (TR/TE, 550/17–20 ms, FOV, 22–24 cm; ST/IG, 5 mm/2 mm; matrix, 384 × 224; flip angle, 15–17°). Contrast enhanced images were obtained after the administration of 0.2 mmol/kg body weight of gadopentate dimeglumine (Magnevist, Schering, Berlin, Germany) or 0.1 mmol/kg of body weight of gadobutrol (Gadovist, Schering) using axial, sagittal, and coronal T1-weighted spin echo sequences for 1.5T (TR/TE, 450–540/11–20 ms; FOV, 22–24 cm; ST/IG, 5 mm/2 mm) or 3D FSPGR T1-weighted sequence for 3T (TR/TE, 6.2/2.6 ms; ST/IG, 1 mm/0 mm with 3 mm reconstruction; FOV, 22 cm; matrix, 512 × 512).

Diffusion-weighted imaging data at 1.5T were obtained by applying three orthogonal diffusion gradients at following parameters: TR/TE, 11000–12000/15–30; FOV, 22–24 cm; ST/IG, 3.5 mm/0 mm; matrix, 128 × 128, b value, 1000 sec/mm^2). Diffusion maps at 3T were obtained from diffusion tensor imaging data set. Diffusion tensor imaging data at 3T were obtained by applying orthogonal diffusion gradients in six different directions and b value of 0 and 1000 s/mm^{-2}(TR/TE, 10000/92.4 ms; FOV, 24 cm; ST/IG, 3.5 mm/0 mm; matrix, 128 × 128). ADC maps were generated from these imaging data.

Image Analysis

CT and ADC map analyses were performed in a blinded manner by one experienced neuroradiologist on a picture archiving and communication system (Centricity, GE Medical System, Milwaukee, WI, USA).

To exclude regions with hemorrhage or typical vasogenic edema, unenhanced T2-weighted and post-contrast T1-weighted MR images were crosschecked. When there are multiple tumors, the largest one was selected for quantitative measurement. In each patient, 6 regions of interest (at least over 20 mm^2) were defined and measured the area of ADC map that corresponded to the solid enhancing portion on postcontrast T1-weighted MR images. The lowest minimum ADC value from among these measurements was selected for statistical analysis. Minimum ADC values of same sized regions in contralateral homologous normal appearing brain parenchyma were measured to calculate ADC ratios.

The highest maximum CT attenuationsin the solid tumor portions were also measured. Regions of necrosis, hemorrhage, or typical vasogenic edema were carefully excluded by examining T2-weighted and postcontrast T1-weighted MR images. CT and MR images were not coregistered. However, the rater carefully compared each pair of CT and MR images to minimize possible errors due to differences in the slice position and scan angle by referring to anatomical landmarks.

Also author compared maximum CT density, minimum ADC and minimum ADC ratio between necrotic PCNSLs (n = 4) and necrotic GBMs (n = 24).

Two radiologists, unaware of final diagnoses and with 12 and 5 years of experience, reviewed all CT and MR images by consensus. They assessed the following imaging features for each tumor: enhancing tumor margin (well defined versus ill defined), tumor enhancement (homogeneous versus heterogeneous), the presence of necrosis, the presence of ventricular wall involvement, the presence of cortical surface involvement, and multiplicity (multiple versus

solitary).

Statistical Analysis

Statistical analysis was performed using commercially available software (PASW Statistics version 17.0; SPSS, Chicago, Ill). Before performing individual analysis, the distributions of data setswere checked for normality. The Mann-Whitney test was used to compare quantitative parameters (maximum CT attenuations, minimum ADC values, and minimum ADC ratios) in the GBM and PCNSL patient groups. The ADC and ADC ratio cutoff value for the differentiation of GBM and PCNSL was determined by receiver operating characteristic (ROC) curve analysis, and areas under the curves (AUCs) were calculated as indices of overall diagnostic accuracy.

Fisher's exact test was used to compare conventional MRI findings in the two groups. Differences were considered significant when P values were < 0.05.

RESULTS

Mean maximum CT attenuation were similar in the PCNSL and GBM groups (mean ± SD; 37.84 ± 6.90 HU versus 37.00 ± 5.54 HU, p = 0.68) (Fig. 1). However, mean minimum ADC and minimum ADC ratio were significantly lower in the PCNSL (595.01 ± 228.28 × 10^{-6} mm^2/s versus 736.52 ± 162.05 × 10^{-6} mm^2/s; p = 0.028, 0.87 ± 0.26 versus 1.14 ± 0.29; p = 0.007, respectively) (Table 1) (Fig. 2).

ROC analysis revealed that the optimal ADC ratio cutoff value for differentiating PCNSL from GBM was 1.006 (sensitivity 85.7%; specificity 69.2%; AUC =

Table 1. Quantitative Assessment of CT Attenuation, Minimum ADC and Minimum ADC Ratios for PCNSL and GBM

	PCNSL (n = 14)	GBM (n = 26)	P value
CT attenuation (HU)*	37.84 ± 6.90***	37.00 ± 5.54	0.68
Minimum ADC (×10^{-6} mm^2/s)	595.01 ± 228.28	736.52 ± 162.05	0.028
Minimum ADC ratio**	0.86 ± 0.26	1.13 ± 0.29	0.007

*HU: Hounsefield Unit.
**ADC ratio: tumor ADC/contralateral normal parenchyma ADC
*** Mean ± standard deviation

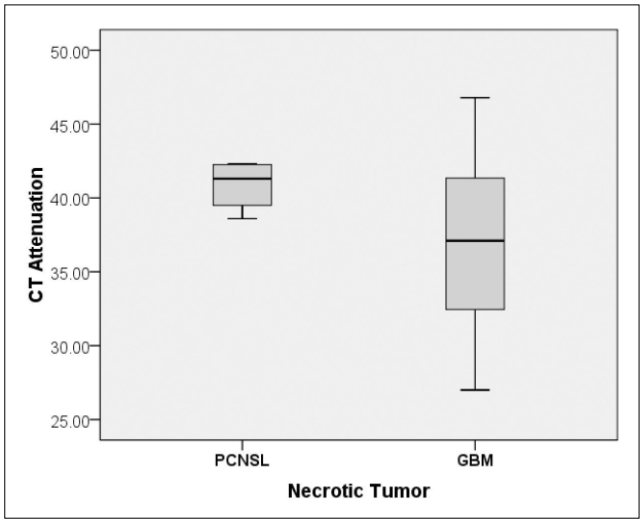

Fig. 1. Boxplot of the CT attenuations of PCNSL and GBM lesions in a subset of necrotic tumors. The line across the box represents the median value. PCNSL and GBM values were not significantly different (p = 0.126). The box ends represent the first and third quartiles, and the end points of each graph represent smallest and largest values.

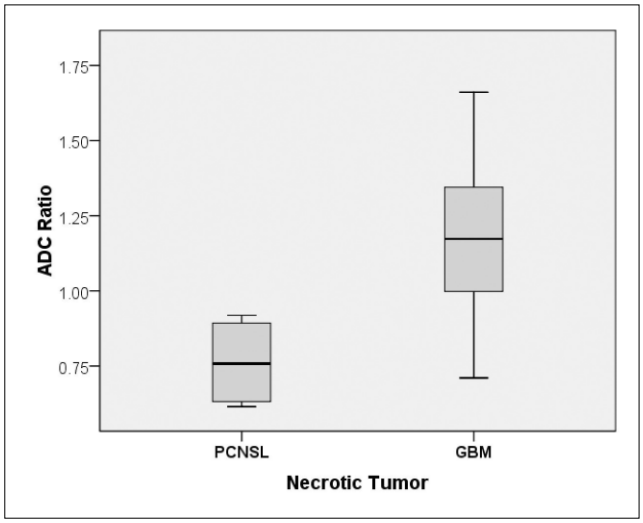

Fig. 2. Boxplot of the minimum ADC ratios of PCNSL and GBM lesions in a subset of necrotic tumors (p = 0.004). The line across the box represents the median value. The box ends represent the first and third quartiles, and the end points of each graph represent smallest and largest values.

0.766; 95% confidence interval, 0.610 – 0.923) (p = 0.006) (Fig. 3).

Although no GBM showed homogeneous enhancement, 35.7% (5/14) PCNSL tumors did. On the other hand, only 28.6% (4/14) of PCNSL tumors but 92.3% (24/26) of GBM tumors exhibited necrosis. No significant intergroup difference was found in tumor margin enhancement or extent of tumor involvement, but PCNSL patients were found to be more likely to have multiple tumors (35.7% versus 7.7%, p = 0.039) (Table 2) (Figs. 4–7).

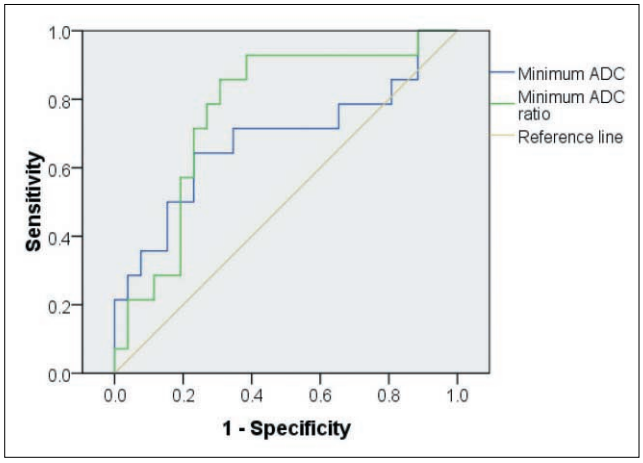

Fig. 3. Minimum ADC and minimum ADC ratios and the differentiation of PCNSL and GBM by receiver operating characteristic curve analysis (For minimum ADC ratios, AUC = 0.766 [95% confidence interval; 0.610–0.923] and p = 0.006, for minimum ADC, AUC = 0.681 [95% confidence interval; 0.491–0.872] and p = 0.061).

Even in a subset of necrotic tumors, mean minimum ADC and ADC ratios were significant different between PCNSL (n = 4) and GBM (n = 24) with lower minimum ADC/ADC ratio for PCNSL (Table 3).

DISCUSSION

In this study, the CT attenuations of PCNSL and GBM tumors were similar, but minimum ADC and minimum ADC ratio values were significantly lower for PCNSL tumors. In addition, the PCNSL- favoring imaging features identified were greater homogeneous enhancement, less frequent necrosis, and tumor multiplicity.

Unlike MRI, which provides information on the chemical composition of tissues, CT provides information on tissue electron density differences in the form

Table 2. Differences between the Imaging Features of PCNSL and GBM Lesions

	PCNSL (n = 14)	GBM (n = 26)	P value
Ill-defined margin	2 (15.3)*	6 (23.1)	0.689
Heterogeneous enhancement	9 (64.3)	26 (100)	0.003
Tumor necrosis	4 (28.6)	24 (92.3)	< 0.001
Ventricular involvement	9 (64.3)	12 (46.2)	0.333
Superficialcortex involvement	7 (50.0)	21 (80.8)	0.071
Deep gray matter involvement	5 (35.7)	21 (80.8)	0.222
Multiplicity	5 (35.7)	2 (7.7)	0.039

*Numbers in parentheses are percentages.

Table 3. Quantitative Assessment of CT Attenuation and Minimum ADC values and Minimum ADC Ratio for PCNSL and GBM in a Subset of Necrotic Tumors

	PCNSL (n = 4)	GBM (n = 24)	P value
CT attenuation (HU)*	40.88 ± 1.75***	36.77 ± 5.16	0.126
Minimum ADC ($\times 10^{-6}$ mm^2/s)	430.3 ± 81.09	761.70 ± 140.99	< 0.001
Minimum ADC ratio**	0.76 ± 0.15	1.18 ± 0.27	0.004

*HU: Hounsefield Unit.
**ADC ratio: tumor ADC/contralateral normal parenchyma ADC
*** Mean ± standard deviation

of Hounsfield Units (HUs). Therefore, CT is highly sensitive to small calcifications and hemorrhages, which contain either high atomic number elements or electron dense materials, such as, iron-containing hemoglobin (19). It has also been suggested that high attenuation within a tumor may be due high packing density of abnormal cells (20). Several previous reports demonstrated that PCNSL tumors are iso- or hyper-attenuated on unenhanced CT images (9–11). However, no previous comparative study has addressed CT attenuation in PCNSL and GBM tumors. Due to recent advances in high-resolution multidetector CT, we considered that quantitative measures of CT attenuation might facilitate the characterization of tumors more cost-effectively than advanced MRI techniques. However, this study shows our hypothesis that CT attenuation measurements might enable the differentiation of PCNSL and GBM was found to be false, which suggests that factors other than tumor cellularity determine tumor CT attenuation values.This result may have been caused by the poor discriminative ability of CT itself, or because maximum CT attenuation was used in the quantitative analysis. We presumed that maximum CT attenuation would better represent the most compactly packed tumor regions than mean CT attenuation, and this may have narrowed the difference between the two groups. We speculate that more elaborative approach such as histogram analysis would provide further information from CT in the future study.

In the present study, mean minimum ADC and minimum ADC ratio were lower in PCNSL than in GBM. In this study, we used minimum ADC values instead of mean ADC because we assumed that minimum ADC would represent the most compact cellular area in the tumor and accordingly better differentiate GBM and PCNSL in terms of cellularity difference (16). In a study by Guo et al., mean ADC of CNS lymphomaswas found to be $870 \pm 270 \times 10^{-6}$ mm²/s, and the mean ADC of high grade gliomas was 1210 ±

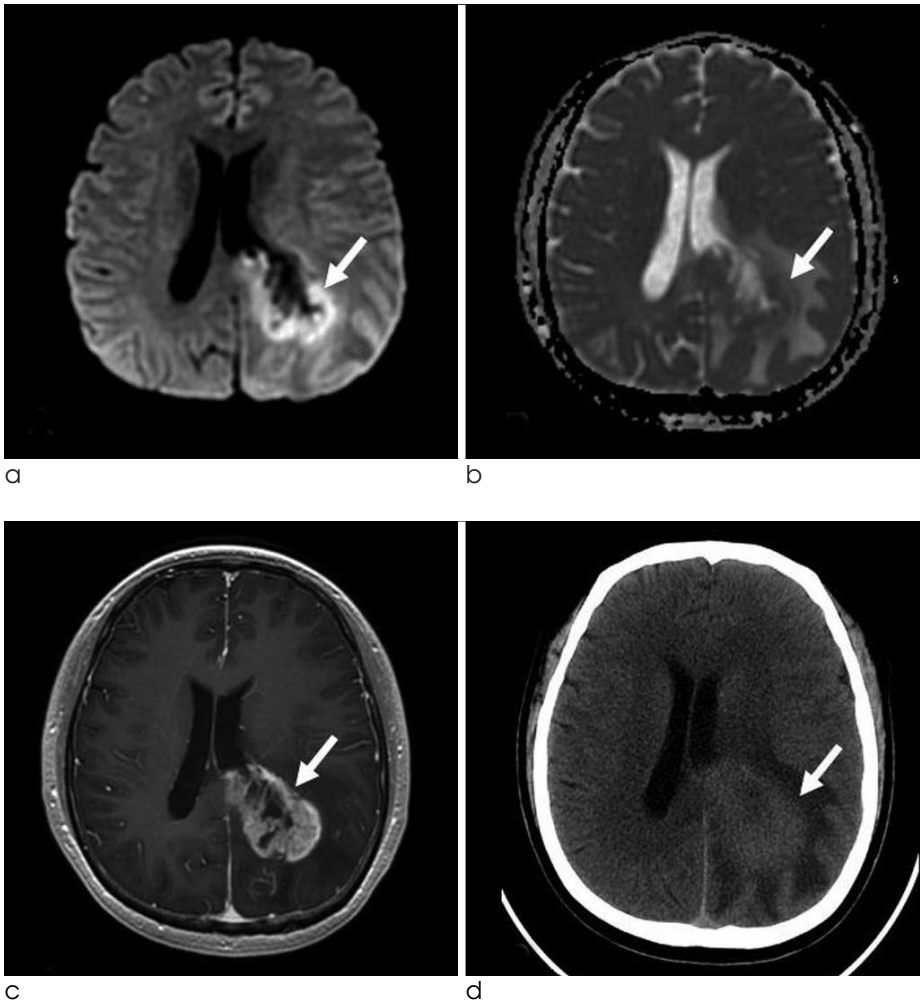

Fig. 4. MR and CT images of 49-year-old man with glioblastoma (GBM).
a. Axial DWI image, **b.** ADC map, **c.** axial post-contrast T1WI image, **d.** axial non-contrast CT. The necrotic enhancing tumor (arrows) is iso-attenuated versus adjacent gray matter on the CT image (maximum CT density; 31.4 HU), hyperintense on the DWI image, and heterogeneously low on the ADC map (minimum ADC; 840×10^{-6} mm²/s).

350×10^{-6} mm²/s (21), whereas according to Toh et al., the mean ADCs of PCNSLs and GBMs were $630 \pm 155 \times 10^{-6}$ mm²/s and $1510 \pm 460 \times 10^{-6}$ mm²/s, respectively (16). Although we used minimum ADC values instead of mean ADC values, our results are in accord with those of these previous studies. Thus, our results show the inverse relationship between ADC values and tumor cellularity by demonstrating lower ADC values in PCNSL, which has higher cellularity and is more compact than GBM.

In the present study, minimum ADC ratio was found to be significantly lower in PCNSL than in GBM with a p value of 0.007, and in previous studies, ADC ratios for PCNSL were also found to be lower than those of GBM (0.63 – 1.15 versus 1.26 – 1.68) (16, 21, 22). In contrast to ADC, which provides a measure of water molecule diffusion in a given voxel, ADC ratio is insensitive to systemic noise or variability (23), and we speculate that this insensitivity caused ADC ratio to better differentiate PCNSL and GBM.

ROC curve analysis showed that a minimum ADC ratio cutoff of 1.006 had a sensitivity of 85.7% for the differentiation of PCNSL and GBM. A previous study on 10 PCNSL and 10 GBM patients found 100% sensitivity and specificity for an ADC ratio cutoff of 1.06 (16). We speculate that the larger number of patients enrolled in the present study might have been responsible for this lower diagnostic accuracy. Combined approach (encompassing DWI, PWI, and MR spectroscopy) rather than single parameter approach is perhaps needed for the differentiation of these two disease entities.

With regard to conventional imaging features, PCNSL tumors were found to more frequently exhibit homogeneous enhancement and to be less prone to necrosis, which agrees well with previous studies (24–26).

Interestingly, we found that tumor involvement sites were similar in the two groups. PCNSL tumors are commonly located at subependymal regions abutting

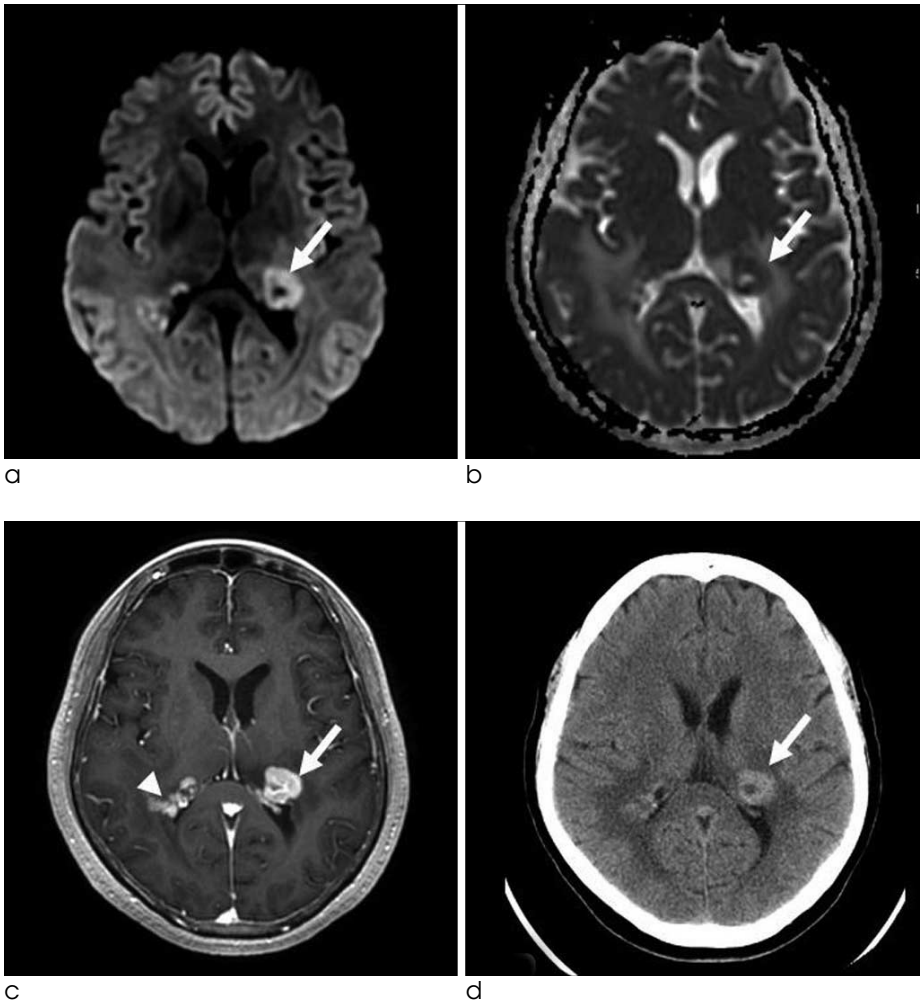

Fig. 5. MR and CT images in 66-year-old man with PCNSL.
a. Axial DWI image, **b.** ADC map, **c.** axial post-contrast T1WI image, **d.** axial non-contrast CT image. This well enhancing tumor with a small region of central necrosis (arrows) was hyperattenuated versus contralateral gray matter on CT images (maximum CT density; 42.3 HU), hyperintense on DWI images, and definitely lower on the ADC map than contralateral normal brain parenchyma (minimum ADC; 377.2×10^{-6} mm²/s). A small enhancing mass is also shown (arrowhead).

the lateral ventricular wall or even invading deep gray matter (27). In one study of 103 focal Non-AIDS PCNSL tumors, 56% were found to abut the lateral ventricular wall (24). Although ventricular wall involvement was not focused on in older studies, a recent study reported that 93% of gliomas contacted at least one region of the lateral ventricular wall (28), whereas another report found that 47% of GBMs involved the lateral ventricular wall (29). In the present study, ventricular wall involvement was observed for 46% of GBMs and 64% of PCNSLs, which suggests that periventricular involvement is not a distinguishing feature for PCNSL. Likewise, other site involvements, such as, of deep gray matter and superficial cortex, were not found to be helpfully differentiating GBM and PCNSL.

In addition, we found that multiplicity was significantly more frequent in PCNSL (35.7%) than in GBM (7.7%). Upto 40% of PCNSL cases reportedly harbor multiple lesions (10, 24, 25, 30, 31). In a recent study, it was reported some GBMs develop from neural stem cells regions and that this process results in the formation of multiple tumors (29). Nevertheless, multiplicity at presentation has been reported to be less frequent in GBM than in PCNSL (10, 24), and the present study shows the same result.

Based on our results, we speculate that irrespective of tumor involvement site, a non-necrotic homogeneously enhanced tumor with a low minimum ADC ratio on DW images is suggestive of PCNSL rather than GBM, and that tumor multiplicity increases the likelihood of PCNSL.

Moreover, even in a subset of necrotic tumors, we found lower minimum ADC and minimum ADC ratio in necrotic PCNSL as compared to necrotic GBM. When we encounter a necrotic enhancing mass on MR imaging, differential diagnosis of this mass could be easier by providing quantitative analysis of minimum ADC and minimum ADC ratio.

Several limitations of the present study bear consideration. First, it is intrinsically limited by its retrospective design. In particular, some PCNSL and GBM patients were not enrolled because they did not undergo imaging, which may have caused selection bias. Second, CT attenuation was measured without co-registering CT and MR images, although the rater made measurements carefully to minimize possible errors. Third, ADC value determinations reportedly show high inter-observer variability, and thus, we also calculated ADC ratios, which according to Sasaki et al.(23), are more suitable for assessing diffusion abnormalities in multicenter studies. Finally, the small number of patients undoubtedly affected the accuracy of the ROC curve analysis.

CONCLUSION

In conclusion, this study shows that CT attenuation values determined on unenhanced CT images do not aid the differentiation of PCNSL and GBM. Nevertheless, we suggest that the minimum ADC and minimum ADC ratios and the presence of homogeneous enhancement, necrosis, and multiplicity aid the differentiation PCNSL and GBM.

References

1. Haldorsen IS, Krossnes BK, Aarseth JH, et al. Increasing incidence and continued dismal outcome of primary central nervous system lymphoma in Norway 1989-2003 : time trends in a 15-year national survey. Cancer 2007;110:1803-1814
2. Haldorsen IS, Espeland A, Larsson EM. Central nervous system lymphoma: characteristic findings on traditional and advanced imaging. AJNR Am J Neuroradiol 2011;32:984-992
3. Shah GD, DeAngelis LM. Treatment of primary central nervous system lymphoma. Hematol Oncol Clin North Am 2005;19: 611-627
4. O'Brien PC, Roos DE, Pratt G, et al. Combined-modality therapy for primary central nervous system lymphoma: long-term data from a Phase II multicenter study (Trans-Tasman Radiation Oncology Group). Int J Radiat Oncol Biol Phys 2006; 64:408-413
5. Elder JB, Chen TC. Surgical interventions for primary central nervous system lymphoma. Neurosurg Focus 2006;21:E13
6. Stupp R, Mason WP, van den Bent MJ, et al. Radiotherapy plus concomitant and adjuvant temozolomide for glioblastoma. N Engl J Med 2005;352:987-996
7. Pichlmeier U, Bink A, Schackert G, Stummer W. Resection and survival in glioblastoma multiforme: an RTOG recursive partitioning analysis of ALA study patients. Neuro Oncol 2008; 10:1025-1034
8. Stummer W, van den Bent MJ, Westphal M. Cytoreductive surgery of glioblastoma as the key to successful adjuvant therapies: new arguments in an old discussion. Acta Neurochir (Wien) 2011;153:1211-1218
9. Koeller KK, Smirniotopoulos JG, Jones RV. Primary central nervous system lymphoma: radiologic-pathologic correlation. Radiographics 1997;17:1497-1526
10. Coulon A, Lafitte F, Hoang-Xuan K, et al. Radiographic findings in 37 cases of primary CNS lymphoma in immunocompetent patients. Eur Radiol 2002;12:329-340
11. Go JL, Lee SC, Kim PE. Imaging of primary central nervous system lymphoma. Neurosurg Focus 2006;21:E4

12. Hartmann M, Heiland S, Harting I, et al. Distinguishing of primary cerebral lymphoma from high-grade glioma with perfusion-weighted magnetic resonance imaging. Neurosci Lett 2003;338:119-122
13. Cianfoni A, Colosimo C, Basile M, Wintermark M, Bonomo L. Brain perfusion CT: principles, technique and clinical applications. Radiol Med 2007;112:1225-1243
14. Zacharia TT, Law M, Naidich TP, Leeds NE. Central nervous system lymphoma characterization by diffusion-weighted imaging and MR spectroscopy. J Neuroimaging 2008;18:411-417
15. Stadnik TW, Chaskis C, Michotte A, et al. Diffusion-weighted MR imaging of intracerebral masses: comparison with conventional MR imaging and histologic findings. AJNR Am J Neuroradiol 2001;22:969-976
16. Toh CH, Castillo M, Wong AM, et al. Primary cerebral lymphoma and glioblastoma multiforme: differences in diffusion characteristics evaluated with diffusion tensor imaging. AJNR Am J Neuroradiol 2008;29:471-475
17. Moon WJ, Choi JW, Roh HG, Lim SD, Koh YC. Imaging parameters of high grade gliomas in relation to the MGMT promoter methylation status: the CT, diffusion tensor imaging, and perfusion MR imaging. Neuroradiology 2012;54:555-563
18. Kim DS, Na DG, Kim KH, et al. Distinguishing tumefactive demyelinating lesions from glioma or central nervous system lymphoma: added value of unenhanced CT compared with conventional contrast-enhanced MR imaging. Radiology 2009; 251:467-475
19. Parizel PM, Makkat S, Van Miert E, Van Goethem JW, van den Hauwe L, De Schepper AM. Intracranial hemorrhage: principles of CT and MRI interpretation. Eur Radiol 2001;11:1770-1783
20. Erdag N, Bhorade RM, Alberico RA, Yousuf N, Patel MR. Primary lymphoma of the central nervous system: typical and atypical CT and MR imaging appearances. AJR Am J Roentgenol 2001;176:1319-1326
21. Guo AC, Cummings TJ, Dash RC, Provenzale JM. Lymphomas and high-grade astrocytomas: comparison of water diffusibility and histologic characteristics. Radiology 2002;224:177-183
22. Horger M, Fenchel M, Nagele T, et al. Water diffusivity: comparison of primary CNS lymphoma and astrocytic tumor infiltrating the corpus callosum. AJR Am J Roentgenol 2009; 193:1384-1387
23. Sasaki M, Yamada K, Watanabe Y, et al. Variability in absolute apparent diffusion coefficient values across different platforms may be substantial: a multivendor, multi-institutional comparison study. Radiology 2008;249:624-630
24. Haldorsen IS, Krakenes J, Krossnes BK, Mella O, Espeland A. CT and MR imaging features of primary central nervous system lymphoma in Norway, 1989-2003. AJNR Am J Neuroradiol 2009;30:744-751
25. Kuker W, Nagele T, Korfel A, et al. Primary central nervous system lymphomas (PCNSL): MRI features at presentation in 100 patients. J Neurooncol 2005;72:169-177
26. Hayakawa T, Takakura K, Abe H, et al. Primary central nervous system lymphoma in Japan--a retrospective, cooperative study by CNS-Lymphoma Study Group in Japan. J Neurooncol 1994;19:197-215
27. Slone HW, Blake JJ, Shah R, Guttikonda S, Bourekas EC. CT and MRI findings of intracranial lymphoma. AJR Am J Roentgenol 2005;184:1679-1685
28. Barami K, Sloan AE, Rojiani A, Schell MJ, Staller A, Brem S. Relationship of gliomas to the ventricular walls. J Clin Neurosci 2009;16:195-201
29. Lim DA, Cha S, Mayo MC, et al. Relationship of glioblastoma multiforme to neural stem cell regions predicts invasive and multifocal tumor phenotype. Neuro Oncol 2007;9:424-429
30. Buhring U, Herrlinger U, Krings T, Thiex R, Weller M, Kuker W. MRI features of primary central nervous system lymphomas at presentation. Neurology 2001;57:393-396
31. Fine HA, Mayer RJ. Primary central nervous system lymphoma. Ann Intern Med 1993;119:1093-1104

대한자기공명의과학회지 16:226-235(2012)

원발성 중추신경계 림프종과 교모세포종의 감별: 전산화 단층 촬영 감쇠계수와 현성 확산 계수의 정량적 분석

[1]건국대학교 의학전문대학원 건국대병원 영상의학과
[2]건국대병원 영상의학과
[3]성균관의과대학 강북삼성병원 영상의학과

이승철[1] · 문원진[1] · 최진우[1] · 노홍기[1] · 박소현[1] · 이정근[1] · 임유정[2] · 정은철[3]

목적: 이 연구의 목적은 기존의 자기공명 영상에 더하여, 전산화 단층촬영 (CT) 감쇠계수와 현성 확산 계수 (ADC)를 정량적으로 측정하는 것이 원발성 중추신경계 림프종과 교모세포종의 감별 진단에 있어 도움이 되는지 알아보고자 함이다.

대상과 방법: 조직학적으로 증명된 26명의 교모세포종 환자와 14명의 림프종 환자가 이 연구에 포함되었다. 종양의 고형부분에서 최대 CT 감쇠계수와 최소 ADC, 그리고, 정상뇌조직과 종양과의 ADC 상대비를 측정하였다. 두명의 신경계 영상의학과 의사가 기존 자기공명 영상의 좋지 않은 경계, 균질한 조영 증강, 괴사의 유무, 종양의 범위, 다발성 여부를 합의하에 정성적으로 분석하였다. Mann-Whitney 검사와 Fisher exact 검사를 이용하여 두 군간의 정량적 분석과 정성적 분석을 비교하였다.

결과: 최대 CT 감쇠계수는 원발성 중추신경계 림프종과 교모세포종에서 비슷하였다 (37.84 ± 6.90 HU 대 37.00 ± 5.54 HU, p=0.68). 그러나, 최소 ADC 와 그 ADC 상대비는 원발성 중추신경계 림프종에서 교모세포종보다 의미있게 낮았다. (595.01 ± 228.28 대 736.52 ± 162.05 10^{-6} mm^2/s; p=0.028, 0.87 ± 0.26 대 1.14 ± 0.29; p=0.007). 원발성 중추신경계 림프종의 경우에 교모세포종에 비하여 균질한 조영증강을 보이고 (p=0.003)과 괴사를 동반하지 않는 경우가 좀더 흔하였다(p 〈 0.001). 괴사를 동반한 종양들만을 비교할 때에도, 최대 CT 감소계수는 의미없었으나, 최소 ADC와 ADC 상대비는 원발성 중추신경계 림프종에서 의미있게 낮았다.

결론: 비록 최대 전산화 단층 촬영 감쇠계수는 원발성 중추신경계 림프종과 교모세포종을 감별진단하는데 있어서는 가치있는 정보를 제공하지 않았지만, 최소 ADC와 ADC상대비 및 일부 기존 영상 소견은 감별진단에 도움이 된다.

통신저자 : 문원진, (143-792) 서울시 광진구 화양동 4-12, 건국대학교병원 영상의학과
Tel. (02) 2030-5499 Fax. (02) 2030-5549
E-mail: mdmoonwj@naver.com, mdmoonwj@kuh.ac.kr